Series: ELECTRONICS, COMPUTERS and ARTIFICIAL INTELLIGENCE – ECAI-2013

Contents

Vol. 5 – No. 1/ 2013 ISSN – 1843 – 2115

Media	IEEE Catalog Number	ISBN
Compliant PDF Files	CFP1327U-ART	978-1-4673-4937-6
DVD	CFP1327U-DVD	978-1-4673-4936-9
Print	CFP1327U-PRT	978-1-4673-4935-2

UNIVERSITY OF PITESTI

Technical sponsorship

IEEE Region 8

IEEE Industry Applications Society

Proceedings of the International Conference on ELECTRONICS, COMPUTERS and ARTIFICIAL INTELLIGENCE – ECAI-2013

Series: ELECTRONICS, COMPUTERS and ARTIFICIAL INTELLIGENCE

Vol. 5 – No. 1/ 2013 ISSN – 1843 – 2115

Media	IEEE Catalog Number	ISBN
Compliant PDF Files	CFP1327U-ART	978-1-4673-4937-6
DVD	CFP1327U-DVD	978-1-4673-4936-9
Print	CFP1327U-PRT	978-1-4673-4935-2

ECAI 2013 - International Conference – 5th Edition
Electronics, Computers and Artificial Intelligence
27 June -29 June, 2013, Piteşti, ROMÂNIA

On the search speed for the extremum seeking control 2d-schemes. Part II – performances estimation

Nicu Bizon[1)2)], Marian Raducu[1)], Mihai Oproescu[1)], Luminita Mirela Constantinescu[1)]
[1)]University of Pitesti, 1 Targu din Vale, Arges, 110040 Pitesti, Romania, nicubizon@yahoo.com ; nicu.bizon@upit.ro; Tel +40 348 453 201, Fax +40 348 453 200
[2)] University Politehnica of Bucharest, 313 Splaiul Independentei, 060042 Bucharest, Romania

Abstract. In this paper a performances analysis of the Extremum Seeking Control (ESC) scheme applied to the dual-inputs single-output (DISO) systems is presented . These ESC 2D-schemes contain two ESC 1D-schemes that have a common input: the output of the DISO system. The performance of the basic high-order ESC (bhoESC) and band-pass filter ESC (bpfESC) 2D-schemes will be analyzed here based on the two orthogonal dither signals. The ratio of the search speeds for these 2D-schemes is estimated analytically during the search speed based on the partial derivatives of the unknown DISO map. The relation of the search speeds ratio related to these partial derivatives and control parameters of the ESC 2D-scheme is shown. The proposed bpfESC 2D-scheme has higher search speed than the bpfESC 2D-scheme, and this is clearly highlighted in this paper based on the simulation performed.

Keywords: nonlinear DISO system, ESC algorithms, ESC performance, ESC 2D-scheme, search speed, tracking accuracy

1. INTRODUCTION

The ESC is a class of adaptive control that deals with regulation to unknown optimal set-points. In general, a nonlinear dynamic plant has an unknown input-to-output map having one ore more extremes (maximums or minimums). The ESC scheme searches the operating set-points that optimize a performance or cost function. In general, it is necessary to use some kind of adaptation algorithms and perturbation methods to search these points in order to track the optimal operating conditions for unknown or partial unknown functions. The ESC schemes have the ability to recover the true unknown values of the parameters necessary in control. It is known that the convergence of parameters to their true values can only be ensured if sufficient excitation is assured in the closed-loops [1, 2].

Two classes of methods, i.e. perturbation-based and model-based ESC schemes, are defined in the literature [2, 3]. These ESC schemes can be also classified as intrinsically or extrinsically perturbed [4]. The extrinsically perturbed methods require a periodical signal (usually names as dither) to be added at the inputs of the nonlinear DISO system. The intrinsically perturbed methods auto-oscillate around the equilibrium point based on delays and hysteresis that appear for some components in the seeking loop. Note that most of the ESC methods proposed to harvest the energy from the hybrid power sources can be considered as intrinsically perturbed [5, 6].

Other view is based on analog and digital optimization approach [2]. The class of the analog optimization-based ESC schemes contains the sinusoidal perturbation and sliding mode-based analog optimization ESC schemes. As it is known, the continuous gradient is the most straightforward and usual approach that has been studied by many specialists [7, 8]. Besides this class, the numerical optimization-based ESC schemes have been recently used successfully [2, 9]. Theoretical stability and convergence results have been presented for both classes in [3]. In general, the performances of the ESC have been demonstrated on single-input single-output (SISO) systems. Different ESC 1D-schemes of sinusoidal perturbation and sliding mode-based were proposed in [8].

As an alternative, the multi-unit optimization method is proposed in [10, 11]. The gradient is computed based on the finite difference between the parallel units that operate with input values differing by a small constant, which can decreases during the searching phase. If the initial value is high enough, then this algorithm is capable to track the global optimum, avoiding blocking in any local optimal points.

In this paper the perturbation-based ESC schemes based on the dither signals will be analyzed [8]. The dither signal is introduced in the ESC loop to achieve the necessary excitation. Note that the problem of determining appropriate parameters of the dither remains open for the nonlinear systems [12].

The design of the dither parameters that satisfies both performance indicators (the search speed and tracking accuracy) cannot be carried out off-line. The proposed bhoESC 1D-scheme includes a forward technique to generate such dither signals in closed-loop. This design guarantees parameters

convergence with a higher tracking accuracy. The bpfESC 2D-scheme is shown in Figure 1 and the design of a dither signal that ensures parameter convergence was presented in Part I of this paper. Two dither components are added on the processed signal in the ESC loop, y_{loop}: (1) the gained dither, s_{dg}, which has variable amplitude during the search phase based on magnitude of first harmonic of y_{BPF} signal, H_1; (2) the minimum dither, s_{dm}, which has a minimum amplitude that improves the tracking accuracy based on the dither persistence.

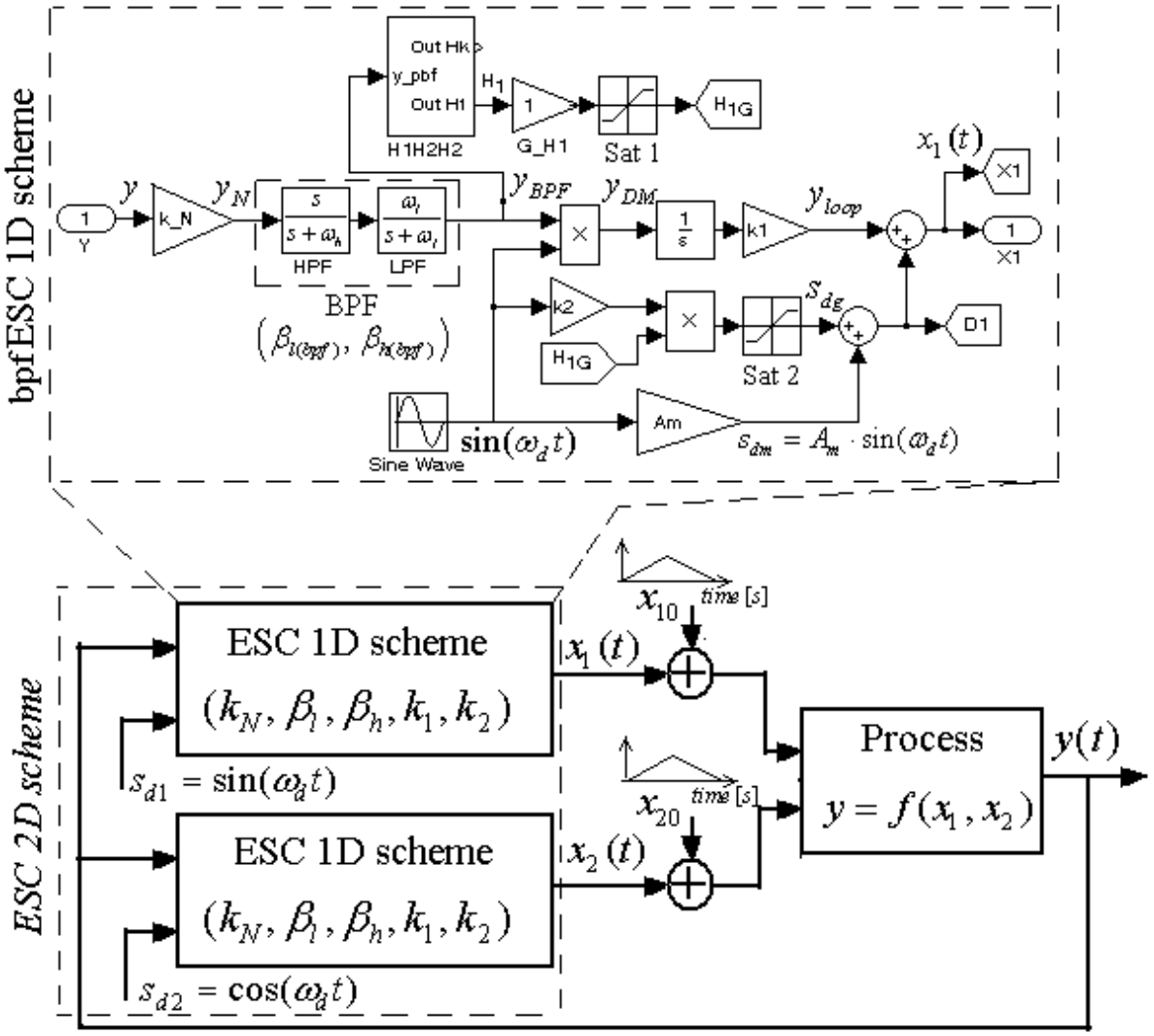

Fig.1. The ESC 2D-scheme operating in closed loop and the bpfESC 1D-scheme

The Part II of this paper is organized as follows. Section 2 presents in brief the ESC 2D-schemes based on orthogonal dither signals and the main results obtained in Part I. Section 3 deals with estimation of the ratio of the search speeds values for the bhoESC and bpfESC 2D-schemes. The comparative results are shown in Section 4 using both ESC schemes applied on three known input-to-output maps. Thus, the theoretical results are illustrated with simulations to validate them. The performance of the bpfESC scheme related to both search speed and tracking accuracy indicators is clearly highlighted in this section based on the simulation performed. The last section concludes the paper.

2. THE EXTREMUM SEEKING CONTROL 2D-SCHEMES BASED ON ORTHOGONAL DITHER SIGNALS

As it was mentioned in first part of this paper, the principle of the ESC for the multi-inputs one-output (MISO) systems [9, 13] is very similar to the SISO case [8]. The orthogonal dither signals are superimposed on both inputs, x_1 and x_2 (see Figure 1) in order to extract the local gradients $\partial f/\partial x_1$ and $\partial f/\partial x_2$. The following notations are shown in Figure 1 and used in next sections:

- k_1 is the loop gain;
- ω_d is the frequency of the dither signal;
- $\omega_l=\beta_l\omega_d$, $3<\beta_l<6$, and $\omega_h=\beta_h\omega_d$, $0<\beta_h<1$, are the cut-off frequencies of the BPF;
- y_N is the signal after normalization to k_N;
- y_{BPF} is the output signal from the BPF;

- H_1 is magnitude of the fundamental harmonic of the y_{BPF} signal;
- G_{H1} is the gain of the H_1 harmonic;
- s_{dg} is the gained dither;
- $k_2H_1G_{H1}$ is the gain of the s_{dg} dither;
- s_{dm} is the minimum dither;
- A_m is the amplitude of the s_{dm} dither;
- y_{DM} is the signal after demodulation;
- y_{loop} is the output signal from the bpfESC loop;
- x_1 and x_2 are the estimation signals of the unknown parameters.

The probing signal is obtained as a response of the LF signals, $x_{1(LF)}$ and $x_{2(LF)}$, applied to the nonlinear map, $y=f(x_1, x_2)$. The normalized probing signal, y_N, is then BP filtered to obtain the y_{BPF} signal.

The local gradients are estimated through demodulation of the y_{BPF} signal, using the same orthogonal dither signals. As it was explained in Part I of this paper, besides the LF components of the demodulation signal, x_{DM}, the gradient from the x_{DM} signal drives an integrator. The outputs of the integrator move the inputs x_1 and x_2 towards their optimal values.

In the standard dither-based ESC scheme, the amplitude of the dither signal is kept constant [14]. It is obvious that higher tracking accuracy can be obtained decreasing the amplitude of the dither. The global extremum can be tracked in certain cases [15].

The amplitude of the dither is reduced in the adaptive manner during the search phase based on the magnitude of the first harmonic of the y_{BPF} signal, H_1. Besides this injected dither, a minimum dither is also injected to maintain the dither persistence during the stationary phase, when the extremum is almost caught. Only this minimum dither appears in the ESC loop. The s_{dg} dither has the amplitude almost zero during the stationary phase because the H_1 magnitude decreases to zero and remains small after the search phase.

This design allows the ESC loops to mitigate the output ripple as the estimation signals, x_1 and x_2, are approaching the optimal values of the unknown parameters that gives the extremum. In addition, the search speed can be set however great, but limited by the saturation blocks to the safe values related to the process under test. These performances can be obtained with advanced adaptive control 2D-scheme based on complex observers included in the ESC loops [9, 16], iterative algorithms [10] or Kalman filters [17].

The proposed design is simple and can be beneficial for example to better solve the problem of tracking an unknown signal source, which is often called source-seeking [18, 19].

The main results obtained in Part I of this paper are shown based on the following assumptions:

- only three components of the Taylor series will be considered;
- the BPF is ideal, having $\beta_{h(bpf)}<1$ and $3<\beta_{l(bpf)}<4$;
- $k_N=1$.

The search speeds, $K_{SS(p)}$, p=1, 2, for the bpfESC 2D-schemes applied to the nonlinear map, $y=f(x_1, x_2)$, were estimated loop based on Taylor series approximation:

$$K_{SS(p)} = \frac{1}{2} D_{(p)} a_{(p)} \cos\left[\varphi_{(p)} + (p-1)\frac{\pi}{2}\right] \cdot \left[1 + \frac{1}{8}\frac{D_3}{D_1}\left(a_1^2 + 2\right.\right. \quad (1)$$

where:

$$D_1 = \frac{\partial f}{\partial x_1}(x_{10}, x_{20}) + \frac{\partial f}{\partial x_2}(x_{10}, x_{20})$$

$$D_2 = \frac{\partial f^2}{\partial x_1^2}(x_{10}, x_{20}) + 2\frac{\partial f^2}{\partial x_1 \partial x_2}(x_{10}, x_{20}) + \frac{\partial f^3}{\partial x_2^2}(x_{10}, x_{20})$$

$$D_3 = \frac{\partial f^3}{\partial x_1^3}(x_{10}, x_{20}) + 3\frac{\partial f^3}{\partial x_1^2 \partial x_2}(x_{10}, x_{20}) + 3\frac{\partial f^3}{\partial x_1 \partial x_2^2}(x_{10}, x_{20}) + \quad (2)$$

$$+ \frac{\partial f^2}{\partial x_2^3}(x_{10}, x_{20})$$

$$\gamma_{sd} = k_1 / \omega_d \quad (3)$$

Note that $K_{SS(p)}$ indicators are time variables based on relationships (1) and (2).

In both cases, the derivatives can be computed during the simulation based on relationship (4):

$$K_{SSp} = \frac{\partial f}{\partial x_p}(x_{10}, x_{20}) = \frac{df}{dt} / \frac{dx_p}{dt}, \quad p = 1, 2 \quad (4)$$

Thus, the signal injected in the loop will be:

$$x_{(p)}(t) \cong K_{SS(p)} \cdot t + (-1)^{p-1} \cdot k_2 H_1 G_{H1} \sin\left[\varphi_{(p)} + (p-1)\frac{\pi}{2}\right]$$

$$+(-1)^{p-1} \cdot A_m \sin\left[\omega_d t + (p-1)\frac{\pi}{2}\right] + x_{(p)(LF)}(t), \quad p = 1, 2 \quad (5)$$

where H_1 is the magnitude of the fundamental harmonic of y_{BPF} signal and G_{H1} is its gain, and the LF components are given by relationships:

$$x_{LF}(t) = \sum_{j=1}^{[\beta_l]} a_j \sin(j\omega_d t + \varphi_j) \quad (6)$$

The integer $[\beta_l]$ was set to 3 based on the assumptions made, but note that this can be set higher than 3 to investigate its effect in dither persistence, and finally in ESC performance.

Estimation of the search speeds in the closed loops of the bhoESC 2D-scheme can be performed in the same manner if the same assumptions are considered, excepting that $\beta_{h(bho)}=0.5$..

The search speeds in the closed loop can be estimated based on:

$$K_{SS(p)(bho)} = \frac{1}{2} D_{(p)} a_{(p)} \cos\left[\varphi_{(p)} + (p-1)\frac{\pi}{2}\right] \cdot \gamma_{sd}\omega_d, \quad p = 1, 2 \quad (7)$$

Thus, the signal injected in the loop will be:

$$x_{1(bho)}(t) \cong K_{SS1(bho)} \cdot t + (-1)^{p-1} \cdot k_2 \sin\left[\varphi_{(p)} + (p-1)\frac{\pi}{2}\right], \quad p = 1, 2 \quad (8)$$

3. ESTIMATION OF THE RATIO OF THE SEARCH SPEEDS VALUES

The ratio of the search speeds values can be estimated based on relationship (19) and (25) as below:

$$R_{SS}(t)=\frac{K_{SSp(bpf)}}{K_{SSp(bho)}}=1+\frac{1}{8}\frac{D_3}{D_1}\left(a_1^2+2a_2^2+2a_3^2\right), \quad p=1,2 \tag{9}$$

Because the magnitude of the LF harmonics (H_1, H_2, and H_3) of the y_{BPF} signals varies during the simulation in the closed loop, these will be estimated using the Fast Fourier Transform (FFT). Thus, relationship (9) used in simulation will be:

$$R_{SS}(t)\cong 1+\frac{1}{8}\frac{D_3}{D_1}\left(H_1^2+2H_2^2+2H_3^2\right), \quad p=1,2 \tag{10}$$

The computing block will use the Matlab-Simulink diagram (see Figure 2) to estimate the absolute ratio of the search speed values based on (10). These diagrams can be also used for comparative tests of the ESC 2D-schemes in closed loop, considering different known DISO maps. In order to validate the analytical results shown above, some simulations were performed for $y_p=f_p(x_1,x_2)=-2+(1-x_1)^{2p}+(1-x_2)^{2p}$, p=1, 2, 3.

4. SIMULATION RESULTS

In all simulation the following parameters are used for the bpfESC 2D-scheme: γ_{sd}=-1 ($k_1=2\pi\gamma_{sd}f_d$), k_2=0.1, $\beta_{h(bpf)}$=0.18, and $\beta_{l(bpf)}$=5.5. Besides these, two values (10 and 100 Hz) are used for the dither frequency (f_d). Also, the effect of the H_1 gain (G_{H1} from Figure 1) to the s_{dg} dither magnitude is highlighted. The saturation blocks (Sat_j, j=1,2) are used in practical cases to limit the search speed value up to the safe limits. The maximum values used here are Sat_{1max}=2 and Sat_{2max}=1, and the minimum values are set to zero. Because the H1 magnitude decreases to zero during the stationary phase, being lower to 10-3, it is necessary to sustain the dither persistence in the closed loop by setting a minimum dither (Am=0.01).

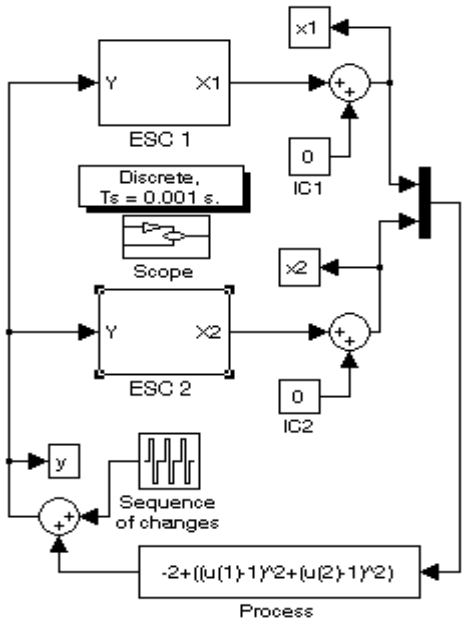

Fig. 2. The diagram for testing the ESC 2D-schemes using different process in the closed loop

The analytical results will be validated by the simulations performed for the basic, $y_p=f_p(x_1,x_2)$, and perturbed process ($y_p=f_p(x_1,x_2)\pm0.5$ or $y_p=f_p(x_1,x_2)\pm1$, p=1, 2, 3).

The partial derivatives for the DISO maps of the basic process considered, $y_p=f_p(x_1,x_2)=-2+(1-x_1)^{2p}+(1-x_2)^{2p}$, p=1, 2, 3, are:

$$\begin{aligned}
&\frac{df}{dx_j}(x_{10},x_{20})=-2p(1-x_{j0})^{2p-1}, \quad p=1,2,3,\ j=1,2\\
&\frac{d^3f}{dx_j^3}(x_{10},x_{20})=-2p(2p-1)(2p-2)(1-x_{j0})^2 \quad p=2,3,\ j=1,2\\
&\frac{d^3f}{dx_j^3}(x_{10},x_{20})=0,\ p=1,\ j=1,2
\end{aligned} \tag{11}$$

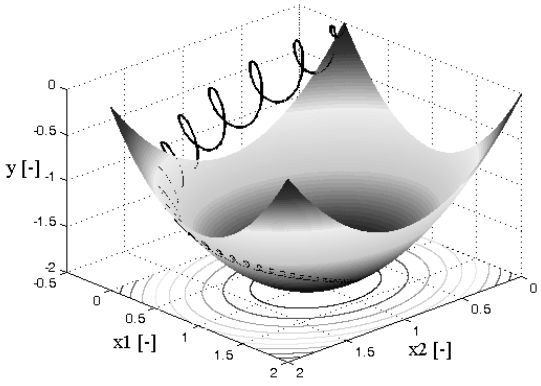

Fig. 3. The 3D view of the search phase for the bpfESC 2D-scheme applied to the process $y=-2-(1-x_1)^2-(1-x_2)^2$: f_d=10 Hz

These relationships were used by the computing block to estimate the D_i parameters, i=1, 2, 3.

First, some simulations are presented in Figure 3 related to the search phase for the bhoESC 2D-scheme (f_d=50 Hz) and a quadratic map of the DISO process: $y=-2-(1-x_1)^2-(1-x_2)^2$. The 2D projections of the search 3D line, $y(t)=-K_{SS(bpf)}t+y_{LF}(t)$, are shown in Figure 4. Note that

$$K_{SS(bpf)} = \sqrt{K_{SS1(bpf)}^2 + K_{SS2(bpf)}^2} = \\ = \gamma_{sd} \cdot \omega_d \cdot \frac{1}{2} D_1 a_1 \cdot \left[1 + \frac{1}{8} \frac{D_3}{D_1} \left(a_1^2 + 2a_2^2 + 2a_3^2 \right) \right] \quad (12)$$

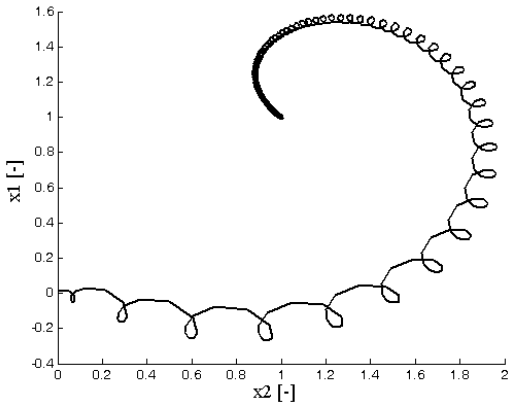

a) projection in (x1, x2) plane

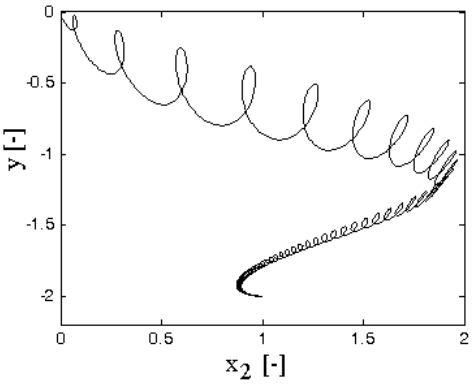

b) projection in (y, x2) plane

Fig. 4. The 2D projections of the search 3D line for the bpfESC 2D-scheme applied to the process $y=-2-(1-x_1)^2-(1-x_2)^2$: f_d=10 Hz

It can be observed in Figure 4a that:

- the y_{LF} signal has LF harmonics with decreasing magnitudes (this can be also seen in Figure 5, second plot);
- the y signal converges to the minimum value with the $K_{SS(bpf)}$ search speed.

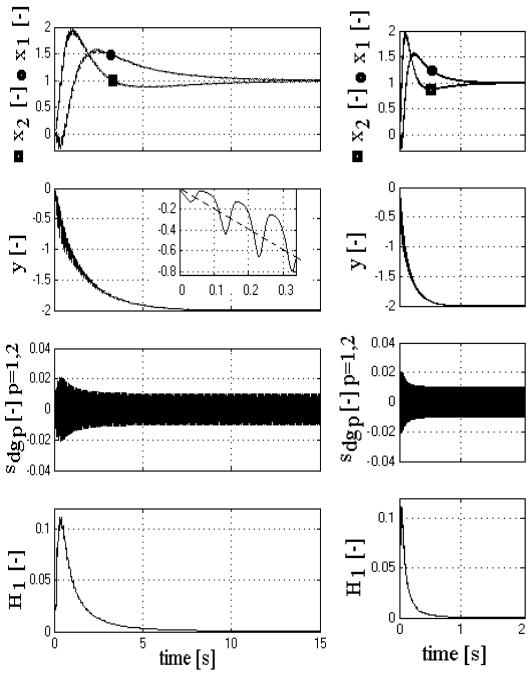

a) f_d=10 Hz b)f_d=100 Hz

Fig. 5. The search phase the bpfESC 2D-scheme applied to the process $y=-2-(1-x_1)^2-(1-x_2)^2$

The initial search speed, $K_{SS0(bpf)}$, can be analytically computed based on relationships (2) and (12):

$$K_{SS0(bpf)} \cong \gamma_{sd} \cdot \omega_d \cdot \frac{1}{2} D_1 a_1 = \\ = (-1) \cdot 10 \cdot \frac{1}{2} \cdot (-4) \cdot 0.1 = 2 \quad (13)$$

The value obtained from simulation can be estimated using Figure 4b:

$$K_{SS0(bpf)} \cong \sqrt{2} \cdot K_{SS20(bpf)} \cong \sqrt{2} \cdot \left| \frac{\partial f}{\partial x_2}(0,0) \right| \cong \\ \cong \sqrt{2} \cdot \left| \frac{\Delta y}{\Delta x_2} \right| \cong \sqrt{2} \cdot \frac{0.7}{0.5} \cong 1.98 \quad (14)$$

or using Figure 5a (see the zoom, where the dashed line represents the average value of y):

$$K_{SS0(bpf)} = \left| \frac{\Delta y}{\Delta t} \right| \cong \frac{0.6}{0.3} = 2 \quad (15)$$

The convergence time is proportional with the dither frequency based on (12), and this is shown in Figure 5. If besides the dither frequency the other parameters used are the same, then the x_1 (●) and x_2 (■) signals have the same shape. A zoom of these signals is shown in Figure 6 during the stationary regime, when (5) become:

$$x_1(t) \cong 1 - A_m \sin(\omega_d t) \\ x_2(t) \cong 1 - A_m \cos(\omega_d t) \quad (16)$$

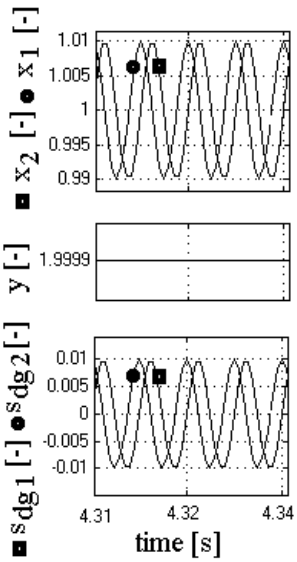

Fig. 6. Zooms of the tracking accuracy the bpfESC 2D-scheme applied to the process $y=-2-(1-x_1)^2-(1-x_2)^2$: f_d=100 Hz

Considering the process $y=-2-(1-x_1)^2-(1-x_2)^2$, the stationary value will be almost constant:

$$y_{st}(t) \cong -2 + A_m^2 \qquad (17)$$

The minimum amplitude of the dither (A_m=0.01; see the plot 3 of Figure 6) sets the stationary error at 10^{-4}. This value is also obtained by simulation (see the plot 2 of Figure 6).

The search phase for the ESC 2D-scheme applied to the perturbed process $y=\pm0.5-2+(1-x_1)^2+(1-x_2)^2$ is shown in Figure 7. The 3D view of the search phase for the perturbed process mentioned above is shown in Figure 8. It can be observed that the tracking of the perturbed values is obtained in short time based on H_1 magnitude that increases during the changes. Considering G_{H1}=1, some zooms of the tracking accuracy are shown in Figure 9 for two levels of perturbation. It can be observed that H_1 magnitude is almost proportional with the level of perturbation. Thus, the gained dithers ($s_{dg(p)}$, p=1,2) will force different search speeds, which are almost proportional with the perturbation levels.

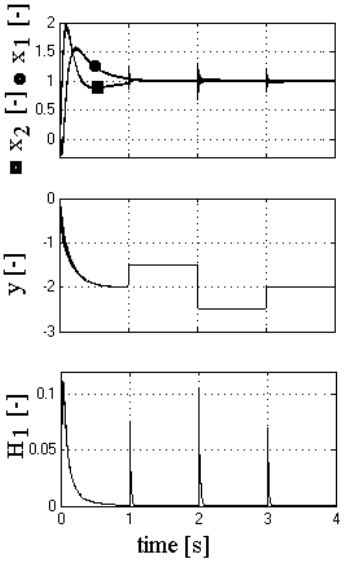

Fig. 7. The search phase for the bpfESC 2D-scheme applied to the perturbed process $y=\pm0.5-2-(1-x_1)^2-(1-x_2)^2$: f_d=100 Hz

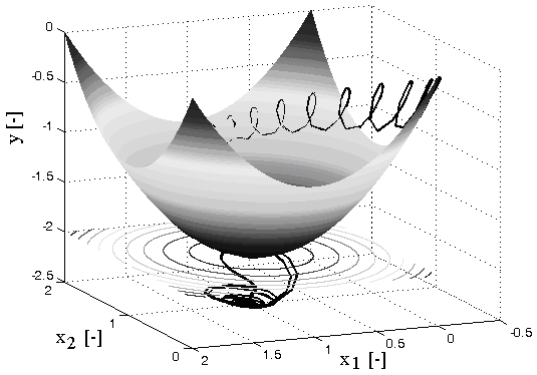

a) The 3D line on the basic process (unperturbed)

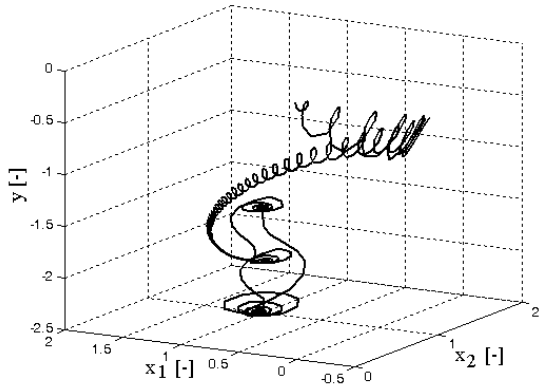

b) The 3D line is shown in a different perspective

Fig. 8. The 3D view of the search phase for the bpfESC 2D-scheme applied to the perturbed process $y=\pm0.5-2-(1-x_1)^2-(1-x_2)^2$: f_d=100 Hz

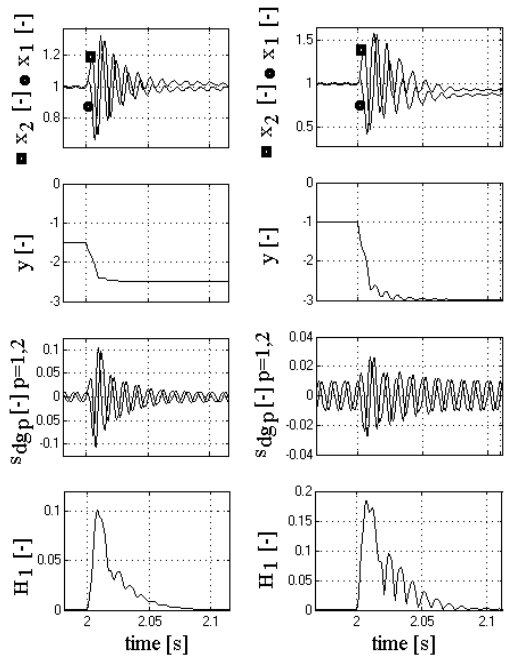

a) $y=\pm0.5-2-(1-x_1)^2-(1-x_2)^2$, G_{H1}=1 b) $y=\pm1-2-(1-x_1)^2-(1-x_2)^2$, G_{H1}=1

Fig. 9. Zooms of the tracking accuracy for the bpfESC 2D-scheme applied to the perturbed process: f_d=100 Hz

Consequently, the values of tracking time are almost equal.

If the G_{H1} parameter is ten times higher than the previous value, then the value of the convergence time (time to track the perturbed values) decreases. Note that this is not in the same ratio (see Figures 9b and 10a). The advantages of the bpfESC scheme in comparison with the bhoESC scheme are shown in Figure 10, too.

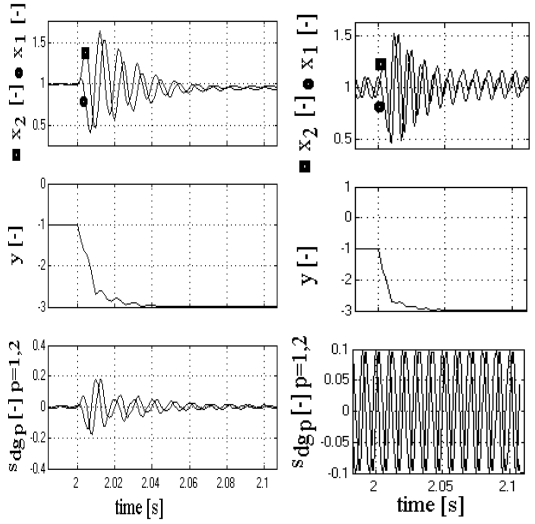

a) bpfESC 2D-scheme, G_{H1}=10 b) bhoESC 2D-scheme ($\beta_{h(bho)}$=0.18, $\beta_{l(bho)}$=0.5)

Fig. 10. Zooms of the tracking accuracy for the ESC 2D-scheme applied to the perturbed process: $y=\pm 1-2-(1-x_1)^2-(1-x_2)^2$, f_d=100 Hz

The simulation results validate the analytical results presented above:

- The search speeds of both bpfESC and bhoESc 2D-schemes are almost the same because the D_3 parameter is zero for the DISO process given by quadratic maps: $y=-2-(1-x_1)^2-(1-x_2)^2$.
- The dithers during the searching phase have the magnitude decreasing to A_m in the bpfESC 2D-scheme, while the dither magnitude is almost constant (set by the k_1 parameter to 0.1) in the bhoESC 2D-scheme.
- This feature mentioned above also highlights that the tracking accuracy of the bpfESC 2D-scheme is better in comparison with the bhoESC 2D-scheme.

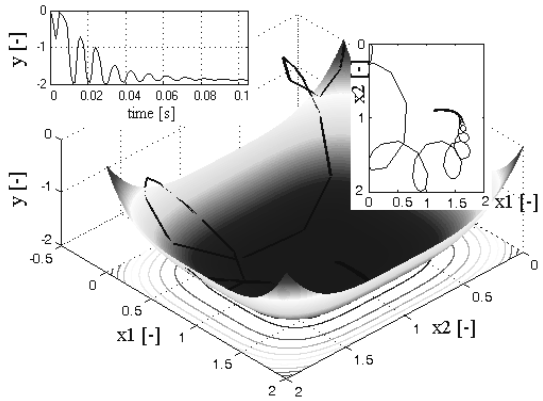

a) applied to the process $y=-2-(1-x_1)^4-(1-x_2)^4$

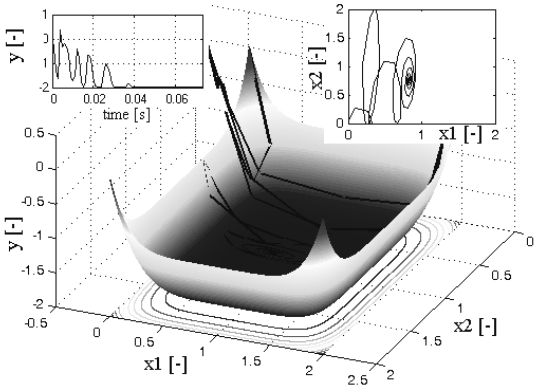

b) applied to the process $y=-2-(1-x_1)^6-(1-x_2)^6$

Fig. 11. The 3D view of the search phase for the ESC 2D-scheme (f_d=100 Hz)

The search speed values can be analytical estimated and validated by simulation based on relationships (13)-(15) for other processes. The 3D view of the search phase for the bpfESC 2D-scheme (f_d=100 Hz): applied to $y_p=f_p(x_1,x_2)=-2+(1-x_1)^{2p}+(1-x_2)^{2p}$, p=2, 3, is shown in Figure 11. Note that the dither has a higher magnitude during the search phase, but this ripple decreases to zero during the stationary phase.

5. CONCLUSION

The proposed design for the bpfESC scheme guarantees high parameter convergence and ensures small ripple during stationary phases. The performance benefits (related to search speed and tracking accuracy) arise from the new design of the bpfESC 2D-scheme.

The simulation shown a high convergence that is guaranteed from any chosen set of initial conditions to a ‘‘small’’ neighborhood of a solution that minimizes the DISO system output. It is obvious that the size of this neighborhood can be made arbitrarily small by decreasing the s_{dm} dither amplitude, and the rate of convergence can be made arbitrarily fast by increasing the γ_{sd} parameter. All the analytical results were validated by simulation using some DISO maps, but in practice the bpfESC 2D-scheme require no knowledge of the system nonlinearity. The promising outcomes from this paper will be exploited in further research in order to apply the bpfESC 2D-scheme in practice.

REFERENCES

[1] Adetola V, Guay M. Parameter convergence in adaptive extremum-seeking control. Automatica 2007;43:105–10.

[2] Zhang C, Ordóñez R. Robust and adaptive design of numerical optimization-based extremum seeking control. Automatica 45 (2009) 634_646

[3] Dochain D, Perrier M, Guay M. Extremum seeking control and its application to process and reaction systems: A survey. Mathematics and Computers in Simulation 2011; 82:369–80.

[4] Leyva R, Artillan P, Cabal C, Estibals B, Alonso C. Dynamic performance of maximum power point tracking circuits using sinusoidal extremum seeking control for photovoltaic generation. Int J of Electronics 2011;98(4):529–42.

[5] Munteanu I, Bratcu AI, Ceanga E. Wind turbulence used as searching signal for MPPT in variable-speed wind energy conversion systems. Renewable Energy 34 (2009) 322–27

[6] Esram, T., Kimball, J. W., Krein, P. T, Chapman, P. L., & Midya, P. Dynamic maximum power point tracking of photovoltaic arrays using ripple correlation control. IEEE Trans Power Electron 2006;21(5):1282–91.

[7] Banavar RN. Extremum seeking loops with assumed functions: estimation and control. International Journal of Control 2003;76:1475-82.

[8] Ariyur KB, Krstić M. Real-time optimization by extremum-seeking control. John Wiley & Sons, NY 2003.

[9] Zhang C, Siranosian A, Krsti¢ M. Extremum seeking for moderately unstable systems and for autonomous target tracking without position measurements. Automatica 2007;43:1832-39.

[10] Azar FE, Perrier M, Srinivasan B. A global optimization method based on multi-unit extremum-seeking for scalar nonlinear systems. Comput Chem Eng 2011;35:456–63.

[11] Woodward L, Perrier M, Srinivasan B. Improved performance in the multi-unit optimization method with non-identical units. Journal of Process Control 2009;19:205–15.

[12] Tan Y, Nesic D, Mareels I. On the choice of dither in extremum seeking systems: a case study. Automatica 2008;44:1446–50.

[13] Ghaffari A, Krstić M, Nešić D. Multivariable Newton-based extremum seeking, Automatica 48 (2012) 1759–1767.

[14] Tan Y, Nesic D, Mareels I. On non-local stability properties of extremum seeking control. Automatica 2006;42(6):889–903.

[15] Tan Y, Nesic D, Mareels I, Astolfi A. On global extremum seeking in the presence of local extrema. Automatica 2009;45:245–51.

[16] Moase WH, Manzie C. Fast extremum-seeking for Wiener–Hammerstein plants, Automatica 2012; 48(10):2433–43.

[17] Gelbert G, Moeck JP, Paschereit CO, King R. Advanced algorithms for gradient estimation in one- and two-parameter extremum seeking controllers. J Process Contr 2012;22:700–9.

[18] Elor Y, Bruckstein AM. Two-robot source seeking with point measurements. Theoretical Computer Science 2012;457:76–85.

[19] Ghods N, Krsti¢ M. Speed regulation in steering-based source seeking. Automatica 2010;46:452-59.